



Role of Compatibilizer in Improving the Properties of PLA/PA12 Blends

Amulya Raj^{1,2*}, Cedric Samuel^{1,2} and Kalappa Prashantha^{1,2,3}

¹ Ecole Nationale Supérieure Mines Telecom Lille Douai, Institut Mines Telecom Lille Douai (IMT Lille Douai), Département Technologie des Polymères et Composites & Ingénierie Mécanique (TPCIM), Douai, France, ² Université de Lille, Lille, France, ³ ACU-Centre for Research and Innovation, Faculty of Natural Science, Adichunchanagiri University, Mandya, India

OPEN ACCESS

Edited by:

Jacqueline Anne Johnson,
University of Tennessee Space
Institute (UTSI), United States

Reviewed by:

M. E. Ali Mohsin,
University of Technology
Malaysia, Malaysia
Debra Puglia,
University of Perugia, Italy

*Correspondence:

Amulya Raj
amulya.raj@imt-lille-douai.fr

Specialty section:

This article was submitted to
Polymeric and Composite Materials,
a section of the journal
Frontiers in Materials

Received: 17 March 2020

Accepted: 25 May 2020

Published: 17 July 2020

Citation:

Raj A, Samuel C and Prashantha K
(2020) Role of Compatibilizer in
Improving the Properties of PLA/PA12
Blends. *Front. Mater.* 7:193.
doi: 10.3389/fmats.2020.00193

Engineering properties of partially-biobased poly(L-Lactide)/poly(amide-12) (PLA/PA12) blends are here addressed using a functional compatibilizer, namely poly(L-Lactide) grafted maleic anhydride (PLA-g-MA). PLA/PA12 blends with compatibilizers are processed using twin-screw extrusion, and the amount of PLA-g-PMA is here optimized with respect to final blend properties such as ductility, impact toughness, and thermal resistance. Blend morphologies depict the enhanced PA12 dispersion into PLA-g-MA with strong interfacial adhesion, in accordance with a compatibilization effect of PLA-g-MA in PLA/PA12 blends. Ductility of the compatibilized blends shows remarkable improvements with the highest ductility close to 290% for an optimized PLA/PA12/PLA-g-MA weight composition (respectively, 69/30/1). The impact strength of compatibilized blends showed a similar two-fold improvement for compatibilized blends. Morphology of injection molded samples revealed finer dispersion and stronger interfaces. The morphology of the transversal section displayed fibrillation of PA12 for PLA-g-MA content up to 2 wt.%. Fibrillation and lower droplet size seemed to play a key role in the improvement of ductility in compatibilized blends. Considerable synergy was detected in the dynamic mechanic analysis of the compatibilized blends. The thermal resistance of the PLA/PA12 blends showed improvement, and this behavior could be due to the formation of copolymer leading to additional interfacial crystallization. This study consequently indicates that PLA-g-MA is an efficient compatibilizer for partially biobased PLA/PA12 blends with potential applications in the automotive and electronic industry.

Keywords: biobased polymers, poly(lactic acid), polymer blends, compatibilization, morphologies, engineering properties

INTRODUCTION

The replacement of petroleum-based polymers to biobased polymers is an immediate need due to the detrimental effects of the former on the environment (Mecking, 2004; Gandini et al., 2011; Mühlaupt, 2013; Harmsen et al., 2014). Among the various biobased polymers, Poly(Lactide) (PLA), also known as Poly(Lactic acid), has gained special attention in the past years owing to its remarkable properties such as renewability (Drumright et al., 2000), biocompatibility (Madhavan Nampoothiri et al., 2010; Farah and Anderson, 2016), transparency (Farah and Anderson, 2016), high modulus (Pang et al., 2010), and biodegradability (Pang et al., 2010; Saeidlou et al., 2012; Hamad et al., 2018; Nofar et al., 2019). These properties led to the commercialization of PLA, thereby making it suitable for various applications such as resorbable sutures

(Pawar et al., 2014), food and beverage packaging (Auras et al., 2004; Ahmed and Varshney, 2011), surgical implants (Pawar et al., 2014), scaffolds (Lasprilla et al., 2012; Lopes et al., 2012), and textiles (Gupta et al., 2007). Despite its propitious properties and applications, the intricacy of implementing PLA in high value or durable applications is restricted due to limitations arising from low melt strength (Nofar et al., 2019), inherent brittleness (Madhavan Nampoothiri et al., 2010; Farah and Anderson, 2016; Hamad et al., 2018), poor impact strength (Farah and Anderson, 2016; Nagarajan et al., 2016), and low heat resistance (Madhavan Nampoothiri et al., 2010; Hamad et al., 2018). Various strategies have been investigated to overcome the drawbacks of PLA, such as toughening mechanisms (Nagarajan et al., 2016; Anderson et al., 2018), copolymerization (Liu and Zhang, 2011; Nagarajan et al., 2016), stereocomplexation of PLA (Li et al., 2016; Tan et al., 2016), addition of nanoparticles and nucleating agents (Shi et al., 2015; Krishnan et al., 2016), and polymer blending (Hamad et al., 2018; Nofar et al., 2019). Among all of the strategies, polymer blending stands out owing to its feasible way to develop new material with versatile and tailor-made properties with the additional benefit of being cost-effective (Utracki and Wilkie, 2014; Mishra et al., 2017; Hamad et al., 2018; Nofar et al., 2019). Blending PLA with engineering polymers is an efficient way to overcome a majority of the limitations of PLA. Over recent years, intensive research is being carried on PLA based blends with engineering polymers such as polycarbonates (Bouzouita et al., 2016), poly(methylmethacrylate) (Samuel and Jean-Marie Raquez, 2013), polyesters (Jiang et al., 2014), and polyamides (Stoclet et al., 2011; Raj et al., 2019). Among the engineering polymers, polyamides stand out, as the blending would enhance the targeted properties of PLA such as low ductility, poor impact strength, and low heat resistance. The improvement in these properties would help in the market penetration of PLA to high-end or durable applications.

Polyamides are engineering polymers with propitious properties such as high ductility, impact strength, stiffness, and higher thermal resistance. In general, PLA/PA blends are immiscible but compatible in nature. Different types of polyamides have been blended with PLA including PA6 (Wang et al., 2010), PA11 (Stoclet et al., 2011), PA6-10 (Pai et al., 2013), PA10-10 (Cailloux et al., 2018), PA10-12 (Raj et al., 2019), and PA12 (Raj et al., 2019). In order to achieve better final properties, it is necessary to improve the compatibility further. One of the classic methods to improve the compatibility is by incorporation of compatibilizers (Utracki and Wilkie, 2014; Zeng et al., 2015). Multifarious compatibilization strategies have been employed in PLA/PA blends by addition of compatibilizers such as polyalkenyl-poly-maleic-anhydride-imide/amide agents, maleic anhydride fraction grafted on polyethylene-octene elastomer, epoxy based compounds, and poly(ethylene-co-glycidyl methacrylate-graft-styrene-co-acrylonitrile) (Wang et al., 2010; Kucharczyk et al., 2012; Dong et al., 2014; Walha et al., 2016; Cailloux et al., 2018; Pai et al., 2019; Rasselet et al., 2019). Walha F et al. studied the effect of multifunctional epoxide (Joncryl ADR[®]-4368) on PLA and PA11 blends, and two routes of compatibilization were investigated: (i) one step

mixing of adding all the components at once to the extruder, (ii) two-step process where initially PLA and Joncryl are premixed and PA11 is introduced later (Walha et al., 2016). Rheological studies revealed good compatibility between the phases and formation of PLA-joncryl-PA11 copolymer was also confirmed. It was observed that both the processes improved the interfacial adhesion, thus reducing droplet size ($<1\mu\text{m}$). Significant improvement in ductility was also observed with the highest being for PLA/PA11(80/20) and 0.7 wt.% of Joncryl ADR[®]-4368 ($\sim 355\%$) (Rasselet et al., 2019). In another interesting study, maleic anhydride grafted on polyethylene octene elastomer was utilized as a compatibilizer in PLA/PA6 (Wang et al., 2010). The blends showed good dispersion with lower domain size, good ductility, and impact strength. This is due to the formation of POE-co-PA6 and POE-co-PLA copolymers, thereby improving the compatibility between the blend components (Wang et al., 2010). There have been some recent studies about reactive compatibilization of PLA/PA11; catalysts such as p-toluenesulfonic acid and titanium isopropoxide have been incorporated to induce ester amide interchange reactions between the blend components (Patel et al., 2014; Gug and Sobkowicz, 2016). Patel et al. observed that the mechanical properties such as ductility, tensile modulus, and toughness of the PLA/PA11 blends were in between the pure polymer's values, suggesting that although the catalyst titanium isopropoxide induced interchange reactions between the polymers, this did not improve the mechanical properties significantly (Patel et al., 2014).

PLA grafted maleic anhydride (PLA-g-MA) has shown to be a potential compatibilizer for PLA blends. It has been incorporated in PLA based starch, poly(ethylene terephthalate glycol) (PETG), and Poly(butylene adipate terephthalate) (PBAT) blends (Zeng et al., 2015). In PLA/starch blends the addition of PLA-g-MA has brought about an improvement in the interface by decreasing the droplet size of the dispersed phase. Significant improvement in tensile strength and ductility were also observed (Huneault and Li, 2007; Wang et al., 2007; Zeng et al., 2015). Additional improvement in morphology, tensile properties, and ductility were found in PLA/PBAT and PLA/PETG blends in the presence of PLA-g-MA as the compatibilizer (Zeng et al., 2015). Maleic anhydride based coupling agents have been previously utilized in PLA/PA blends as mentioned above (Wang et al., 2010; Kucharczyk et al., 2012). However, there are no significant studies of PLA-g-MA as a compatibilizer in the PLA/PA blend system. It would be interesting to observe the effect of PLA-g-MA as a compatibilizer on PLA/PA12 blend properties and investigate if similar improvement in morphology and ductility can be obtained.

In our previous work, we have reported various PLA blends with long-chain aliphatic polyamides. It was found that PA12 showed the best compatibility with PLA with low interfacial tensions, good dispersion, and exceptional mechanical properties (ductility $>170\%$ for 40 wt.% PA12), good impact properties, and thermal resistance (Raj et al., 2019). Hence, in an attempt to obtain further improvement thermal resistance and mechanical properties we present the effect of PLA-g-MA as a compatibilizer on the properties of PLA/PA12 blends.

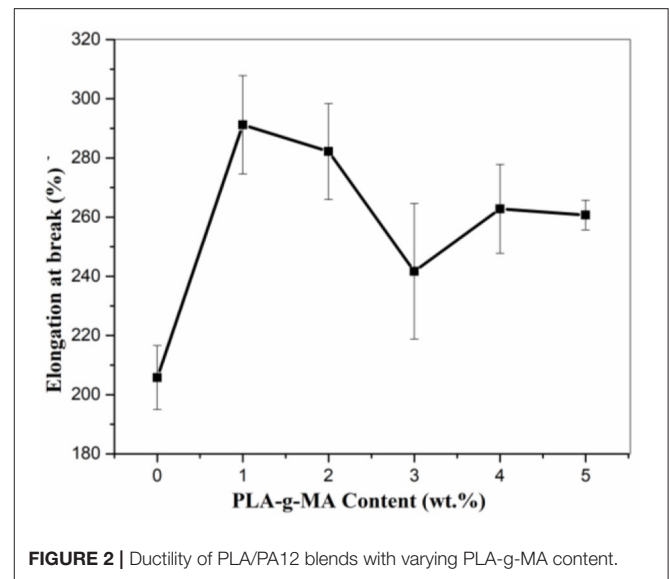
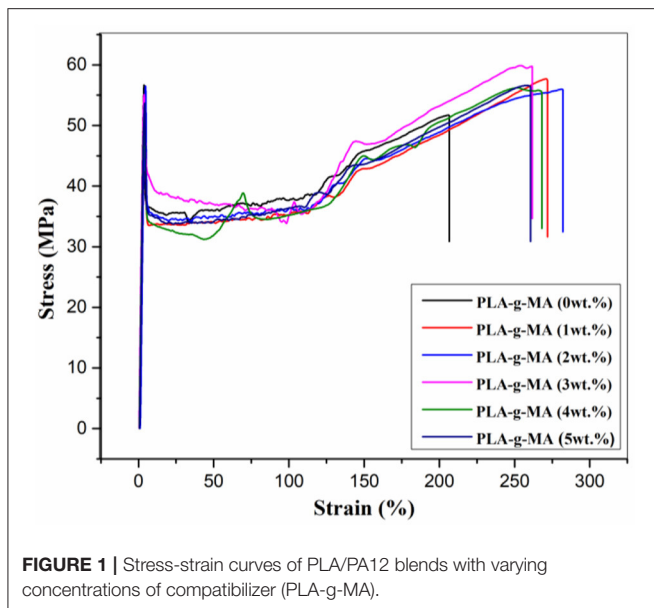
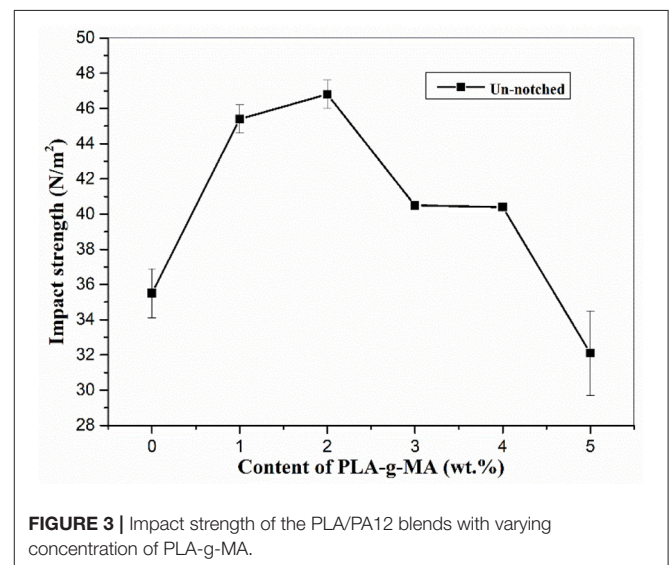


TABLE 1 | Stress at yield, strain at break, and impact strength for as-produced PLA/PA12/PLA-g-MA blends.

PLA/PA12/ PLA-g-MA compositions	Stress at yield (MPa)	Strain at break (%)	Young's Modulus modulus (GPa)	Impact strength (un-notched) (kJ/m ²)
100/0/0	66.6 (1.8)	3.4 (1.5)	2.9 (0.06)	18.1 (0.6)
0/100/0	39.5 (1.2)	138.3 (2.3)	1.4 (0.05)	No break
70/30/0	56.5 (1.6)	153.0 (3.3)	2.2 (0.06)	28.3 (0.7)
69/30/1	55.3 (1)	291.2 (16.6)	2.1 (0.05)	45.4 (0.8)
68/30/2	53.9 (2.4)	282.2 (16.2)	2.1 (0.04)	46.8 (0.8)
67/30/3	52.8 (3.1)	268.7 (22.9)	2.1 (0.09)	40.5 (0.2)
66/30/4	52.4 (4.5)	268.2 (15)	2.1 (0.1)	40.4 (0.2)
65/30/5	53.7 (0.9)	260.7 (5.04)	2.0 (0.3)	32.1 (2.4)



MATERIALS AND METHODS

Materials

Poly(L-lactide) (PLA, grade 4032D, biobased content 100%, density 1.24 g/cm³, melting temperature 171°C, melt volume index 6.5 cm³/10 min at 210°C, according to manufacturer data) was procured from NatureWorks[®], USA. Poly(amide-12) (PA12, grade Rilsamid AESNO, density 1.01 g/cm³, melting temperature 179°C, melt volume index 2.1 cm³/10 min at 235°C, according to manufacturer data) was supplied by Arkema, France. PLA and PA12 were used as received in the pellet form. PLA grafted maleic anhydride (PLA-g-MA) was kindly provided to us by the University of Mons and the preparation method can be referred in the research work published by Quintana et al. (2016). It has a maleic anhydride content of 0.45%.

Processing of PLA/PA12 Blends

Before compounding, the polymers were dried thoroughly under vacuum at 80°C for 8 h to remove any traces of moisture in the materials. PLA/PA12/PLA-g-MA (wt.% 70/30/0, 69/30/1, 68/30/2, 67/30/3, 66/30/4, 65/30/5) were processed by twin-screw extrusion using a Haake Rheomex PTW 16 OS twin-screw extruder (Thermoscientific, Germany, screw diameter 16 mm, L/D 40). The average speed maintained during extrusion was 80 rpm, with a total mass flow rate close to 500 g/h and a mean residence time of ~2 min. The barrel temperature regulation is carried out on 10 zones and the temperature profile was maintained constant for all experiments (200–205–210–210–210–210–210–200–185°C), from the hopper to the die. The extrudates were cooled in a water bath and pelletized. The

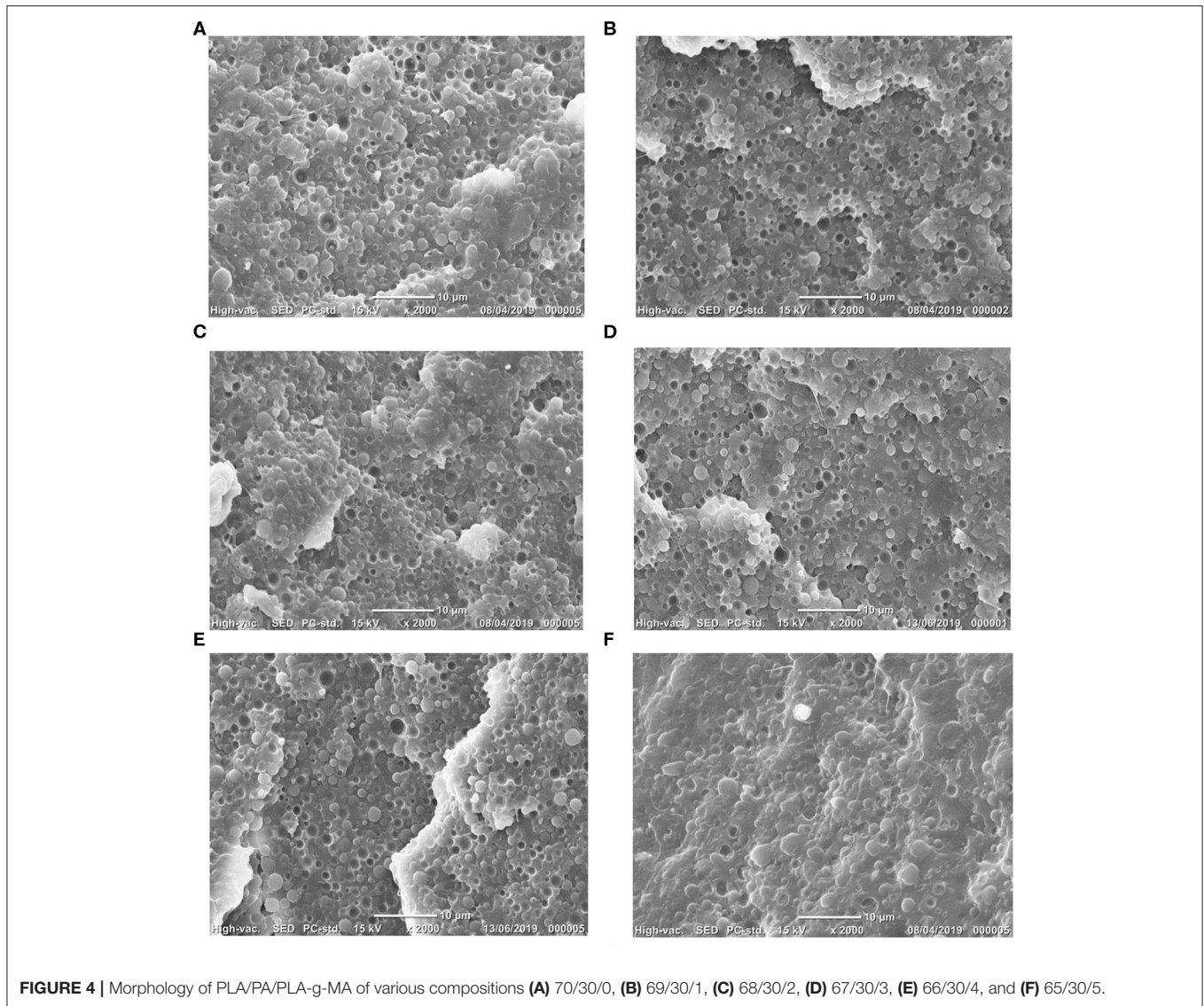


FIGURE 4 | Morphology of PLA/PA/PLA-g-MA of various compositions **(A)** 70/30/0, **(B)** 69/30/1, **(C)** 68/30/2, **(D)** 67/30/3, **(E)** 66/30/4, and **(F)** 65/30/5.

pellets were dried at 80°C under vacuum overnight. After thorough drying pellets were used for the following molding processes. Pristine polymers were also extruded through a similar procedure.

Tensile test specimens were prepared by following the ISO-527-1 standards. The dimensions of the specimens are as follows: gauge length 50 mm, width of 5 mm, and thickness of 1.5 mm. They were processed by injection-molding using a Haake Minijet II molding machine. The following processing conditions were used for the preparation of injection-molded specimens: mold temperature 45°C, chamber temperature 215°C, injection pressure 550 bar, cooling time 5 s. Impact specimens were prepared by injection molding (Babyplast 6/10P, Spain). The processing parameters maintained during the preparation of samples were as follows: the temperature ranged from 200 to 210°C and the mold temperature was around 35–50°C. The injection and the consecutive pressure

were 60 and 80 bars, respectively, with a cooling time of 10 s. Specimens for morphological characterization were processed by compression-molding, and Dolouet molding press was utilized for this process. The parameters and conditions were used for all compression-molded specimens (melt temperature: 205°C, melting time and low-pressure cycle: 8 min, high pressure cycle: 5 min).

Methods

Scanning Electron Microscopy (SEM)

The morphology of the compression-molded PLA/PA blends was examined using a scanning electron microscope (SEM, Neoscope II, JEOL, magnification $\times 60,000$). Prior to the observation of morphologies, the specimens were cryo-fractured in liquid nitrogen. These fractured samples were then metallized by gold sputtering under vacuum in order to make them conductive. Droplet sizes of the dispersed phase were measured

TABLE 2 | Number-average and volume-average PA12 droplet diameters (D_n and D_v), PA droplet size polydispersity (I_p) with standard deviation in brackets of PLA/PA12/PLA-g-MA blends (compression molded samples).

Blend	D_n (μm)	D_v (μm)	I_p
70/30/0	1.1 (0.1)	1.4 (0.03)	1.2
69/30/1	1 (0.06)	1.2 (0.05)	1.2
68/30/2	1 (0.04)	1.2 (0.06)	1.2
67/30/3	1.3 (0.1)	1.5 (0.09)	1.1
66/30/4	1.3 (0.1)	1.6 (0.06)	1.2
65/30/5	1.5 (0.07)	1.8 (0.05)	1.2

by image analysis using Image J software. The analysis was done on 50 droplets at least followed by size classification into 7/8 classes. The volume and number average droplet radius diameters (D_v , D_n) with the droplet diameter polydispersity (I_D) were calculated using Equations 1–3. The standard deviations of the size of the droplets were presented by measuring two samples.

$$D_n = 2 \times \frac{\sum n_i \times R_i}{\sum n_i} \quad (1)$$

$$D_v = 2 \times \frac{\sum n_i \times R_i^3}{\sum n_i \times R_i^3} \quad (2)$$

$$I_D = \frac{D_v}{D_n} \quad (3)$$

with D_n the droplet number-average diameter, D_v the droplet volume-average diameter, R_i the average droplet radius of the i -class, and n_i the number of droplets into the i -class.

Tensile and Impact Tests

Tensile tests were carried out on PLA/PA blends and neat polymers in a tensile test machine (Instron 3110, U.K) and a 1 kN force cell to obtain stress–strain curves. Tensile properties were determined in accordance with ISO 527-1 (pre-load of 0.5 N, strain rate 1 mm/min for Young's modulus, and 10 mm/min for general properties). Five dumbbell specimens were tested at the least. Charpy un-notched impact tests were carried out as per ISO 179-1 standard by using a pendulum impact machine (Model 5101, Zwick, Germany) at 25°C and 50% RH and impact energy of 7.1 J. The reported values were evaluated as averages of seven specimens.

Dynamic Mechanical Analysis (DMA)

The dynamic mechanical analysis of the specimens was carried out on dual cantilever beam in the flexion mode (DMA+150, MetraviB, France). The samples were heated over a temperature range (25–130°C) at a heating rate of 2°C/min and frequency of 10 Hz. Two rectangular specimens were tested at the least. The cold crystallization peak of PLA was avoided by annealing the specimens at 110°C for 6 h. The approximate thermal resistance of blends which could correspond to heat deflection temperature (HDTa and HDTb) at two different storage moduli

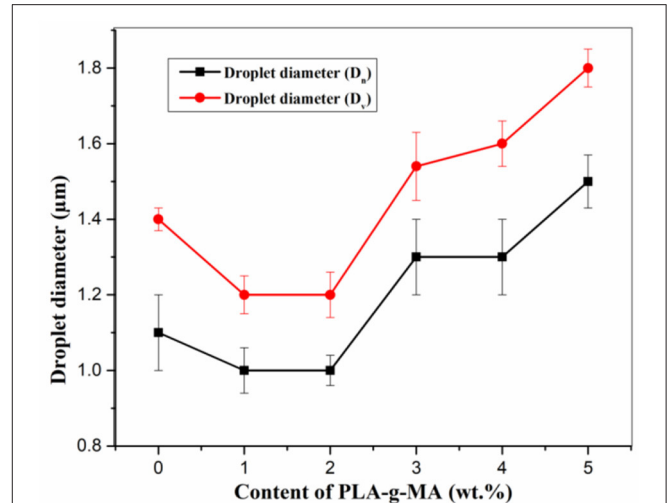


FIGURE 5 | Emulsification curve of PLA/PA12 blends with varying PLA-g-MA content.

(400 and 250 MPa), respectively, were evaluated by the DMA graphs. A method was partially implemented in several studies (Takemori, 1979; Spinella et al., 2016). These storage modulus values were first calibrated using known values on polyamides and temperatures where storage modulus drops down to 400 and 250 MPa were named $T_{400\text{MPa-HDTa}}$ and $T_{250\text{MPa-HDTb}}$, respectively (Battagazzore et al., 2016).

Differential Scanning Calorimetry (DSC)

Differential scanning calorimetry (DSC Mettler Toledo) was utilized to measure the PLA crystallinity of pristine PLA and PLA/PA12/PLA-g-MA blends. The evaluation was performed on injection-molded specimens following an annealing step. The DSC evaluation was carried out under nitrogen atmosphere and a single heating scan at 10°C/min was used for this purpose. PLA melting temperatures and associated enthalpy of fusion (T_m and ΔH_m) were obtained and the PLA crystallinity index ($X_c\text{-PLA}$) was assessed according to Equation 4. It should be noted that PLA crystallinities were normalized to the amount of PLA in PLA/PA blends

$$X_{c\text{-PLA}} = \frac{\Delta H_{m\text{-PLA}} - \Delta H_{cc\text{-PLA}}}{\Delta H_m^0} \times 100 \quad (4)$$

with X_c is the degree of crystallinity, $\Delta H_{m\text{-PLA}}$ the melting enthalpy of PLA, $\Delta H_{cc\text{-PLA}}$ the cold crystallization enthalpy of PLA during heating, and ΔH_m^0 the melting enthalpy of fusion for 100% crystalline PLA (93 J/g) (Jia et al., 2017).

Extraction/Separation Experiments by Centrifugation

The PLA matrix and the PA12 dispersed phase of PLA/PA12/PLA-g-MA blends were selectively extracted/separated by PLA dissolution followed by centrifugation in centrifugal rotary machine (Hettich D7200, Germany). Predetermined weights (~1 g) of extruded pellets of PLA/PA12 blends were dissolved in dichloromethane (1 mL)

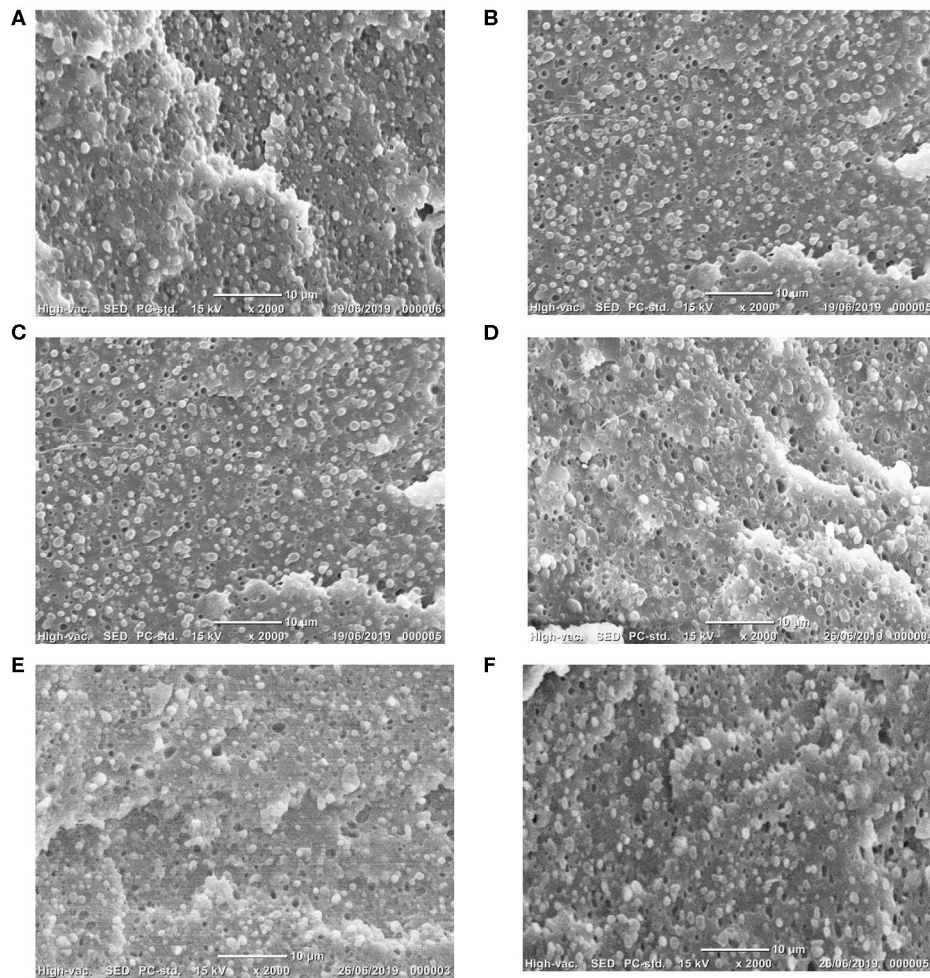


FIGURE 6 | Cross-sectional SEM analysis of injection-molded PLA/PA12/PLA-g-MA blends (A) 70/30/0, (B) 69/30/1, (C) 68/30/2, (D) 67/30/3, (E) 66/30/4, and (F) 65/30/5.

and acetone (9 mL). The solution was then submitted to centrifugation. Centrifugation time was set 1 h at a rotation speed of 4,000 rpm. After every centrifugation cycle, the dissolved phase was carefully transferred in a beaker and a fresh solvent system (dichloromethane/acetone 1:9) was added to the centrifugation tube containing the insoluble PA12 fraction. The dissolution–centrifugation was repeated 5–6 times. The PLA solution and settled PA12 particle were dried for 48 h prior to further characterizations.

Fourier Transform Infrared Studies

The chemical structure of the neat PLA, PA12, and extracted PA12 phase was evaluated by Fourier transform infrared (FTIR) spectroscopy (Nicolet 380 FTIR, ThermoScientific, France). The analysis was carried out on the extracted PA12 phase in reflection mode. The absorption spectra were logged utilizing a microscope in reflection or transmission mode. The range of spectra employed is $4,000\text{--}800\text{ cm}^{-1}$ by the resolution of 16 cm^{-1} and utilizing 62 scans.

RESULTS AND DISCUSSIONS

Mechanical Properties

The major emphasis of this study was to investigate the effect of compatibilizer on engineering properties such as mechanical and the same under dynamic load. The blends were processed by injection molding and subjected to tensile testing; the related stress-strain curves are plotted in **Figure 1**. The values of stress at yield, elongation at break, and Young's modulus evaluated by tensile tests are tabulated in **Table 1**. The poor ductility of PLA (3.4%) drastically improved by the addition of 30 wt.% PA12 (153%), indicating good compatibility as confirmed in our previous studies (Raj et al., 2019). PLA-g-MA was incorporated in the blends to observe the potential evolution of compatibility and its effect on mechanical properties.

There was a significant improvement in the ductility with the addition of PLA-g-MA as a compatibilizer in PLA/PA12 blends as can be seen in **Figure 1**. Even at low concentrations of PLA-g-MA (1 wt.%), the improvement in ductility ($\approx 291\%$)

TABLE 3 | Number-average and volume-average PA12 droplet diameters (D_n and D_v), PA droplet size polydispersity (I_p) with standard deviation in brackets of PLA/PA12/PLA-g-MA blends.

Blend	D_n (μm)	D_v (μm)	I_p
70/30/0	1.1 (0.09)	1.3 (0.09)	1.2
69/30/1	0.94 (0.07)	1.06 (0.04)	1.1
68/30/2	0.83 (0.04)	0.9 (0.03)	1.1
67/30/3	0.9 (0.05)	1 (0.03)	1.1
66/30/4	0.9 (0.03)	1.02 (0.04)	1.1
65/30/5	0.96 (0.06)	1.04 (0.09)	1.1

is noteworthy. Hence, it could be said that very little amount of PLA-g-MA is adequate to further improve the compatibility, leading to higher ductility.

However, with further increase in content of PLA-g-MA, a minor decrease in the ductility is observed, the lowest ductility obtained for 5 wt.% of PLA-g-MA (260%). The decrease in ductility is linear with PLA-g-MA content, and it should be noted that the decrease in ductility is not drastic, suggesting that even at higher concentrations there is no interfacial debonding leading to poor ductility.

The values of Young's modulus and stress at yield are in the range of 2.0–2.1 GPa and 54–55 MPa, respectively for all the compositions. These values are intermediate of PLA (2.9 GPa, 67 MPa) and PA12 (1.4 GPa, 39.5 MPa) in accordance with previous studies of PLA and PA (Stoclet et al., 2011; Nuzzo et al., 2014; Rashmi et al., 2015).

The evolution of ductility with varying content of PLA-g-MA in PLA/PA12 blends is plotted in **Figure 2**. The content of PLA-g-MA required to improve the ductility remarkably (291%) is as low as 1 wt.%, and a further increase in the content does not have an incremental effect on ductility.

The impact strength of the injection molded blend samples was evaluated. The Charpy un-notched impact strength of the PLA/PA12/PLA-g-MA blends are tabulated in **Table 1**. The variation of impact strength with different concentrations of PLA-g-MA is plotted in **Figure 3** for a clear depiction of the influence of compatibilizer on PLA/PA blends. The toughening effect of PA12 can be clearly seen in the PLA/PA12 (70/30, 28.3 kJ/m²) blends without compatibilizer. It is noteworthy to observe that with the incorporation of PLA-g-MA there is further increase in impact strength, suggesting the positive effect of compatibility in blends. The maximum impact strength (45 kJ/m²) achieved was for the blends containing 2 wt.% of PLA-g-MA. Further addition of PLA-g-MA in blends showed a slight linear decrease in impact strength and the least value (32.1 kJ/m²) being for 5 wt.% of PLA-g-MA. Ductility and toughness are considered important properties for durable applications. The addition of compatibilizer (PLA-g-MA) in PLA/PA12 blends has a positive effect on ductility and toughness. Hence, it can be said that these blends could be suitable for high value applications with high ductility requirements.

The SEM images of the blends with various amounts of compatibilizer could give us a better understanding of the

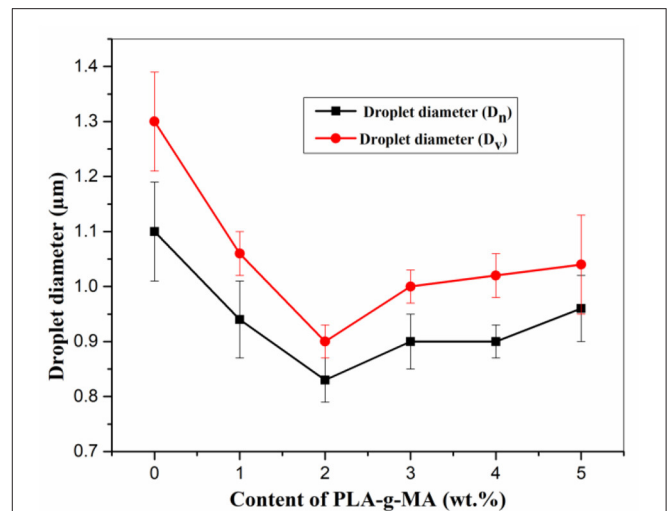


FIGURE 7 | Droplet diameter of PLA/PA12 blends with varying concentration of PLA-g-MA.

improvement in properties. The morphologies of compressed and injection molded samples of blends and their correlation with mechanical properties are discussed in the following section.

Morphology

PLA/PA12/PLA-g-MA blend samples were compressed and cryogenically fractured; the SEM images of the same are represented in **Figure 4**. The continuous phase is represented by PLA, and PA12 droplets are dispersed in the PLA matrix (**Figure 4**). The blends displayed good dispersion and the dispersion seems to improve with the addition of PLA-g-MA. The D_n , D_v , and I_p are tabulated in **Table 2**, where it can be observed that the polydispersity index remains constant (≈ 1.2) for all compositions.

The domain size of PA12 decreased with the addition of PLA-g-MA ($\approx 1 \mu\text{m}$) until 2 wt.%; further addition increased the droplet size of PA12. The droplet size of PA12 in blends with the highest concentration of PLA-g-MA (5 wt.%) is $\approx 1.5 \mu\text{m}$, and it could be said that the blends reached saturation at 2 wt.% of PLA-g-MA as further increase in the content results in the bigger droplet size of dispersed phase (PA12) (**Figure 5**). The reduction in the droplet size could be related to compatibilization effect of PLA-g-MA on PLA/PA12 blends at the interface, resulting in decrease of coalescence of droplets. However, the interfacial adhesion is strong between the blend components and remains unaltered with the increase in concentration of PLA-g-MA, suggesting no interfacial debonding occurs even at higher concentrations of PLA-g-MA.

Morphology of Injection Molded Samples-Correlation With Mechanical Properties

Morphology of injection-molded samples was observed to get an in-depth knowledge of the effect of compatibilizer on the

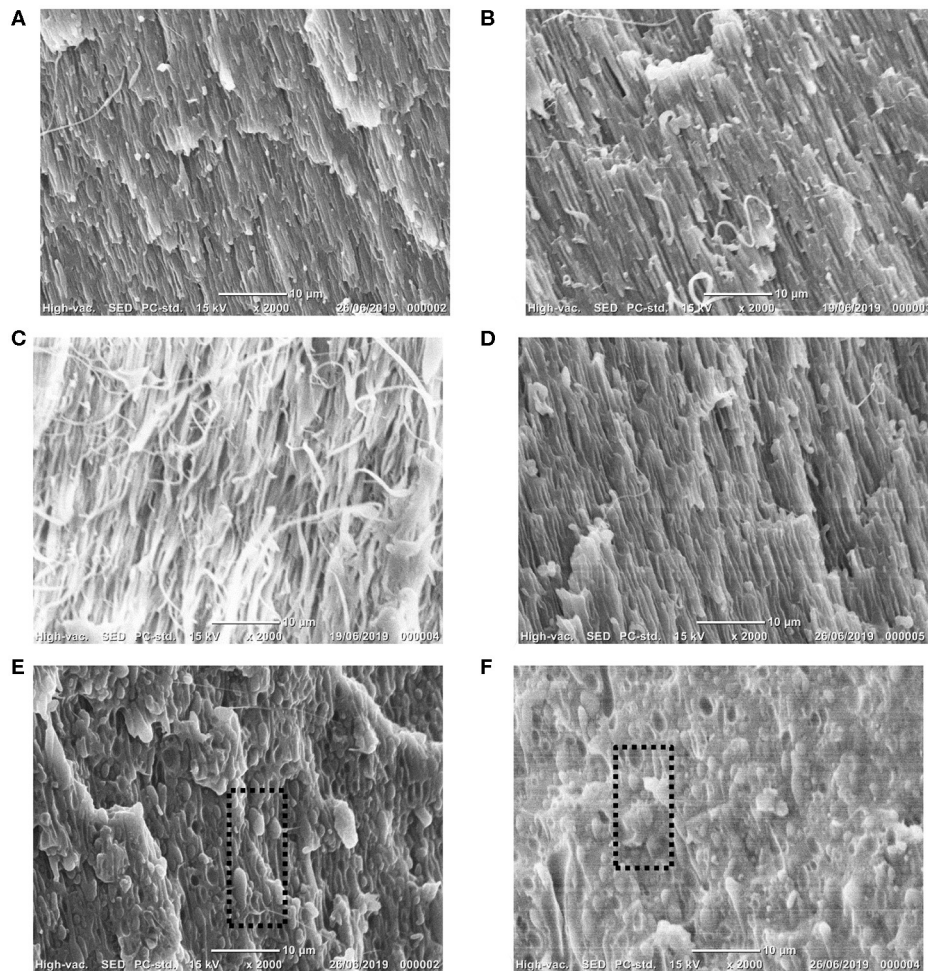


FIGURE 8 | Transversal section SEM analysis of injection-molded PLA/PA12/PLA-g-MA blends **(A)** 70/30/0, **(B)** 69/30/1, **(C)** 68/30/2, **(D)** 67/30/3, **(E)** 66/30/4, and **(F)** 65/30/5.

mechanical properties of the blends. The SEM images of the transversal and cross-sectional part of the injection-molded samples are depicted in **Figures 6, 8**. The blends display a fine dispersion of PA12 droplets in PLA matrix. D_n , D_v , and I_p of the PLA/PA12/PLA-g-MA blends are tabulated in **Table 3**. The droplet diameter of PA12 ranges from micronic to submicronic with lowest being for 2 wt.% of PLA-g-MA ($0.8\ \mu\text{m}$), and the polydispersity index is ≈ 1.1 for all the blend compositions.

The evolution of droplet diameter as a function of PLA-g-MA content has been plotted in **Figure 7**. It can be clearly seen that the droplet diameter decreases linearly up to 2 wt.% and an increment in the droplet size was noticed with a further increase in PLA-g-MA concentration. The lower droplet diameters, better interfacial adhesion, and stronger interface between the blend components of injection molded samples (**Figure 6**) when compared to compression molded samples (**Figure 4**) could be the reason for higher ductility in blends (Stoclet et al., 2011;

Walha et al., 2016; Raj et al., 2019). It is interesting to observe that for injection molded samples, the droplet size of 5 wt.% PLA-g-MA ($0.96\ \mu\text{m}$) is lower than PLA/PA12 (70/30) ($1.1\ \mu\text{m}$); this fine dispersion of PA12 droplets even at higher concentration of PLA-g-MA could be the reason for the ductility behavior of the blends at 5 wt.% of PLA-g-MA (260%). The fibrillation of PA12 can be observed in the **Figures 8A–D**.

At higher concentrations of PLA-g-MA the fibrillation of PA12 appears to be hindered as can be observed in the highlighted area in **Figures 8E,F**. This could be due to higher concentration of compatibilizer at the interface limiting the formation of elongated PA12 in the injection molded samples (Mantia et al., 2017; Kuzmanović et al., 2018). This behavior of hindered elongation of PA12 could be related to the slightly lower ductility and impact strength values (260%, $32\ \text{kJ/m}^2$) obtained for the blends containing a higher concentration of PLA-g-MA (5 wt.%). To further study the interactions between the compatibilizers and the polymers, FTIR was performed.

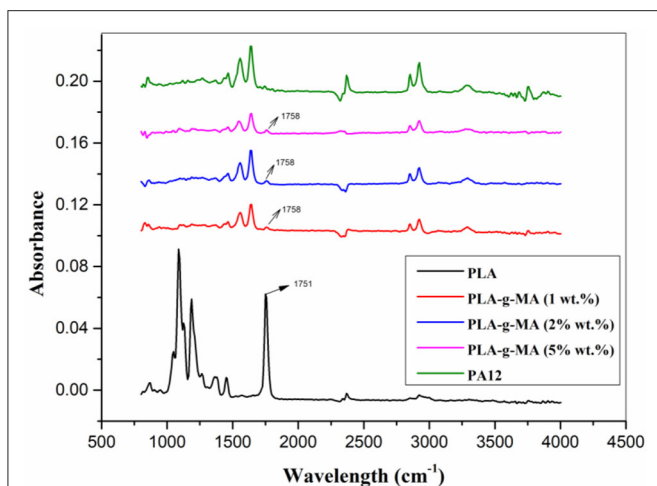


FIGURE 9 | FTIR studies of PLA/PA12 blends with varying content of compatibilizers.

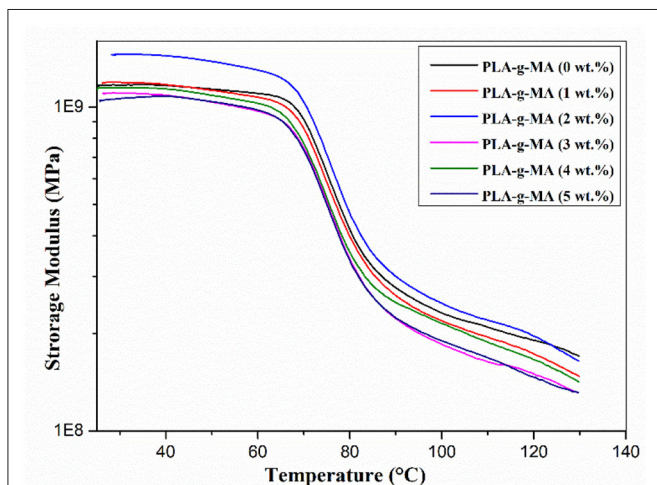


FIGURE 10 | Storage modulus as a function of the temperature of PLA/PA12 blends with varying content of PLA-g-MA (wt.%).

FTIR Studies

FTIR was performed to study the possible grafting or copolymer formation between PLA and PA due to the presence of compatibilizer. FTIR was done on the extracted PA12 phase from centrifugation. The relative absorptions at 3,286 and 1,751 cm^{-1} correspond to characteristic stretching vibration absorptions of NH amide groups and C=O ester groups of PA12 and PLA, respectively, (Figure 9) (Feng and Ye, 2010; Ogunniran et al., 2012). The existence of the absorption peak corresponding to the carbonyl group of PLA in the extracted phase of PA12 could be considered as evidence to grafting/copolymer formation in low amounts.

Additionally, the absorption peak of the carbonyl group appears to have shifted from 1,751 to 1,758 cm^{-1} for the blend (Figure 9), suggesting hydrogen bonding interaction

TABLE 4 | Thermal properties of PLA/PA12 blends with varying content of PLA-g-MA.

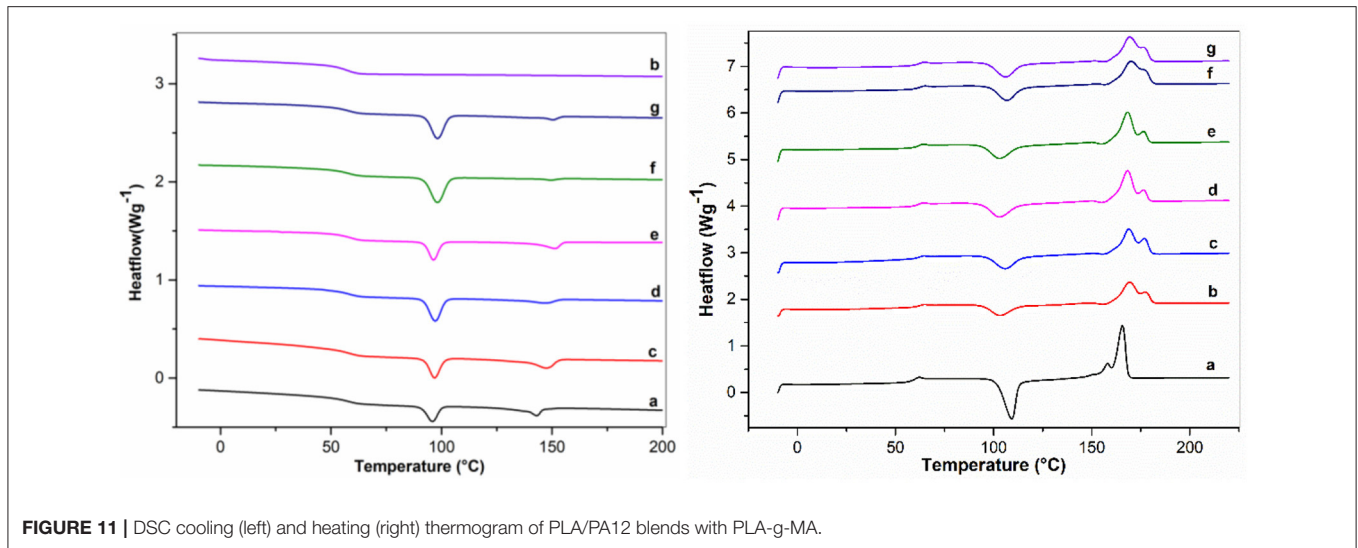
PLA/PA12/ PLA-g-MA compositions	$T_{400\text{Mpa}}$ HDT _A (°C)	$T_{250\text{Mpa}}$ HDT _B (°C)	Melting point (°C)		T_g (°C)
			(PLA)	(PA12)	
100/0/0	78 (0.5)	84 (1)	168.0	-	61.0
70/30/0	81 (2.5)	95 (3.7)	169.4	177.8	64.7
69/30/1	80 (0.5)	92 (0.0)	168.6	176.7	64.7
68/30/2	84 (1)	99 (0.5)	168.3	176.4	64.2
67/30/3	80.5 (1)	86 (1)	168.1	176.4	64.2
66/30/4	81 (1.5)	89 (1.5)	169.3	176.7	64.2
65/30/5	79 (1)	86 (0.8)	169.8	177.2	64.0

between the molecules of PLA and PA12 resulting from the grafting/copolymer formation of PLA and PA12 (Feng and Ye, 2010). Overall the enhancement of mechanical properties could be due to the combined effects of grafting, PA12 droplet size, and PA12 fibrillation. However, PA12 fibrillation and PA12 droplet size could be a predominant factor for the improvement in ductility and toughness. The amount of PLA grafting could represent a key parameter to control in order to avoid losing PA12 fibrillated structures.

(Thermo)mechanical Properties

Thermomechanical properties including thermal resistance or heat deflection temperature (HDT) are prominent for high value applications. Thermomechanical properties were evaluated using DMA to obtain the evolution of the storage modulus/loss factor with temperature.

The HDT ($T_{400\text{MPa}}\text{--HDT}_a$ and $T_{250\text{MPa}}\text{--HDT}_b$) were subsequently extracted from storage modulus with a specific experimental procedure previously reported (Raj et al., 2019). The HDT of PLA/PA12 blends under load was evaluated by dynamic mechanical analysis. The influence of varying concentrations of compatibilizer on the HDT of blends was investigated through these tests. The variation of storage modulus with temperature has been plotted in Figure 10. It is important to note that the blends were annealed at 110°C to eliminate the cold crystallization of PLA. The storage modulus (E') gradually decreases with temperature with a classical drop for temperatures higher than 70°C associated with the glass transition/ α -relaxation of PLA (Figure 10). The α -relaxation temperature of PLA/PA12(70/30) blends is noticed close to 70°C. Higher storage modulus is observed for 2 wt.% of PLA-g-MA blends in comparison with the other compositions. This behavior is still indeterminate but an additional PLA crystallization at PLA/PA12 interface could induce a significant increase in PLA crystallinity (Zhang and Thomas, 2011; Srithep et al., 2013; Raj et al., 2019). The impact of the concentration of compatibilizer on storage modulus is not significant in the glassy state. However, in rubbery state ($T > 70\text{--}80^\circ\text{C}$), a prominent influence of 2 wt.% of PLA-g-MA is observed. The other concentrations did not show this synergism.



Such thermomechanical modifications in the glassy/rubbery state can be correlated with HDT/thermal resistance improvements. Heat deflection temperature ($T_{400\text{MPa-HDTa}}$ and $T_{250\text{MPa-HDTb}}$) of blends were subsequently evaluated from DMA graphs and tabulated in **Table 4**. PLA/PA12/PLA-g-MA blends exhibited similar HDT values as uncompatibilized blends with an exception of PLA-g-MA 2wt.%. Significant improvement of HDT was observed for 2wt.% of PLA-g-MA ($84^{\circ}\text{C-T}_{400\text{MPa-HDTa}}$ and $99^{\circ}\text{C-T}_{250\text{MPa-HDTb}}$). The HDT values do not display similar trends that were observed in mechanical properties. However, above 2 wt.% of PLA-g-MA, decrease in HDT values was observed with the least being for 5 wt.% ($79^{\circ}\text{C-T}_{400\text{MPa-HDTa}}$, $86^{\circ}\text{C-T}_{250\text{MPa-HDTb}}$).

In conclusion, the addition of compatibilizer to the PLA/PA12 blends is beneficial to improve thermal resistance with a considerable increase in the thermal resistance for 2 wt.% of PLA-g-MA. Similar to tensile and impact properties, the optimum content of PLA-g-MA to enhance thermal resistance of PLA/PA12 blends is found to be at 2 wt.%.

Differential scanning calorimetry was performed on PLA/PA12 blends to investigate several thermal properties such as glass transition temperature, melting temperature, and cold crystallization behavior. The T_g of all the blends is around 64°C , which is an intermediate value between PLA and PA12. This is a typical additive rule behavior and it could be said that the compatibilizer does not affect T_g of the blend. It can be observed in heating thermograms (**Figure 11**) that the melting point of the blends with compatibilizer is slightly lower than that of uncompatibilized blends, the reaction of anhydride group of PLA-g-MA and amino group PA12 could be the reason, thereby suggesting a formation of copolymer at the interface. This copolymer could be a hindrance to the motion of segments causing difficulty in polymer chain arrangement (Wang et al., 2010). However, there is a minor increase in the melting point at 4 and 5 wt.% of PLA-g-MA. The cooling thermograms of the blends show a typical droplet and bulk crystallization behavior

of PLA/PA blends (Stoclet et al., 2011; Rashmi et al., 2015; Raj et al., 2019). The temperature at which droplet crystallization occurs remains almost unaltered (97°C) for uncompatibilized and compatibilized blends. However, the bulk crystallization behavior shows an effect of compatibilizer (PLA-g-MA), with an increase in temperature of bulk crystallization as the content of PLA-g-MA increases. This might be due to larger droplets or the copolymer at interface delaying the bulk crystallization of the blends.

CONCLUSIONS

The major emphasis of this study is to examine the compatibilization effects of PLA-g-MA on PLA/PA12(70/30) blends in a twin-screw extruder. Various concentrations of PLA-g-MA were incorporated in the blends to assess the optimum content of compatibilizer required to achieve properties. The positive effect of PLA-g-MA is evident in morphology, mechanical properties, and thermal resistance. Concerning the mechanical properties, remarkable improvement in ductility was observed in the blends with varying content of PLA-g-MA. The impact properties of the compatibilized blends showed similar trends, and the toughening behavior of PA12 is observed. Based on this study the content of PLA-g-MA required to improve the mechanical properties (ductility and impact strength) is 1–2 wt.%. Morphology of the compression molded blend samples with different concentrations of PLA-g-MA revealed fine dispersion of PA12 in the PLA matrix with a strong interface and good interfacial adhesion. To get a better in-depth understanding of the improvement in mechanical properties, the morphology of injection molded specimens was examined. The cross-sectional SEM images revealed finer dispersion, stronger interface, and better interfacial adhesion when compared to compression molded samples. This could be the reason for the improvement in ductility and toughness of the blends.

Transversal sections of injection molded samples were also examined to assess the relation between fibrillation of PA12 and mechanical properties of the blends; the fibrillation of PA12 is evident in the SEM images. However, for higher content of PLA-g-MA hindrance in the fibrillation might be due to the higher concentration of PLA-g-MA at the interface, impeding the elongation of PA12. FTIR studies were also done to study the probable grafting and its correlation with mechanical properties. The absorption peak corresponding to carbonyl group of PLA in the extracted phase of PA12 could be considered an indication of grafting/copolymer formation. This could be considered as a contributing factor for the improvement in ductility. The influence of compatibilizer on PLA/PA12 blends on the thermal resistance of the blends (HDT) was not as significant as mechanical properties. In conclusion, PLA-g-MA is a suitable compatibilizer for PLA/PA12 blends. Remarkable improvement in ductility was observed and considerable improvement in toughness and heat resistance was attained. These blends could be well suited for durable applications which require high ductility and toughness. Further studies related to particular applications are required to discover the apt application for these blends.

REFERENCES

- Ahmed, J., and Varshney, S. K. (2011). Polylactides—chemistry, properties and green packaging technology: a review. *Int. J. Food Prop.* 14, 37–58. doi: 10.1080/10942910903125284
- Anderson, K. S., Schreck, K. M., Hillmyer, M. A., and Schreck, K. M. (2018). Toughening polylactide. *Polym. Rev.* 48, 85–108. doi: 10.1080/15583720701834216
- Auras, R., Harte, B., and Selke, S. (2004). An overview of polylactides as packaging materials. *Macromol. Biosci.* 4, 835–864. doi: 10.1002/mabi.200400043
- Battegazzore, D., Salvetti, O., Frache, A., Peduto, N., De Sio, A., and Marino, F. (2016). Thermo-mechanical properties enhancement of bio-polyamides (PA10.10 and PA6.10) by using rice husk ash and nanoclay. *Compos. A Appl. Sci. Manuf.* 81, 193–201. doi: 10.1016/j.compositesa.2015.11.022
- Bouzouita, A., Samuel, C., Notta-Cuvier, D., Odent, J., Lauro, F., Dubois, P., et al. (2016). Design of highly tough poly (l -lactide)-based ternary blends for automotive applications. *J. Appl. Polym. Sci.* 133:n/a–n/a. doi: 10.1002/app.43402
- Cailloux, J., Abt, T., Santana, O., and Carrasco, F. (2018). Effect of the viscosity ratio on the PLA / PA10. 10 bioblends morphology and mechanical properties. *exPRESS Polym. Lett.* 12, 569–582. doi: 10.3144/expresspolymlett.2018.47
- Dong, W., Cao, X., and Li, Y. (2014). High-performance biosourced poly(lactic acid)/polyamide 11 blends with controlled salami structure. *Polym. Int.* 63, 1094–1100. doi: 10.1002/pi.4618
- Drumright, R. E., Gruber, P. R., and Henton, D. E. (2000). Polylactic acid technology. *Adv. Mater.* 12, 1841–1846. doi: 10.1002/1521-4095(200012)12:23<1841::AID-ADMA1841>3.0.CO;2-E
- Farah, S., and Anderson, D. G. (2016). Physical and mechanical properties of PLA, and their functions in widespread applications — a comprehensive review. *Adv. Drug Deliv. Rev.* 107, 367–392. doi: 10.1016/j.addr.2016.06.012
- Feng, F., and Ye, L. (2010). Structure and property of polylactide/polyamide blends. *J. Macromol. Sci. B* 49, 1117–1127. doi: 10.1080/00222341003609179
- Gandini, A., Rodríguez, H., Rahman, M., Rogers, R. D., Labidi, J., Hedenqvist, M. S., et al. (2011). The irruption of polymers from renewable resources on the scene of macromolecular science and technology. *Green Chem.* 13, 1061–1083. doi: 10.1039/c0gc00789g
- Gug, J., and Sobkowicz, M. J. (2016). Improvement of the mechanical behavior of bioplastic poly(lactic acid)/polyamide blends by reactive compatibilization. *J. Appl. Polym. Sci.* 133:n/a–n/a. doi: 10.1002/app.43350
- Gupta, B., Revagade, N., and Hilborn, J. (2007). Poly(lactic acid) fiber: an overview. *Prog. Polym. Sci.* 32, 455–482. doi: 10.1016/j.progpolymsci.2007.01.005
- Hamad, K., Kaseem, M., Ayyoob, M., Joo, J., and Deri, F. (2018). Polylactic acid blends: the future of green, light and tough. *Prog. Polym. Sci.* 85, 83–127. doi: 10.1016/j.progpolymsci.2018.07.001
- Harmsen, P. F. H., Hackmann, M. M., and Bos, H. L. (2014). Green building blocks for bio-based plastics. *Biofuel. Bioprod. Bior.* 8, 306–324. doi: 10.1002/bbb.1468
- Huneault, M. A., and Li, H. (2007). Morphology and properties of compatibilized polylactide/thermoplastic starch blends. *Polymer (Guildf).* 48, 270–280. doi: 10.1016/j.polymer.2006.11.023
- Jia, S., Yu, D., Zhu, Y., Wang, Z., Chen, L., Fu, L., et al. (2017). Morphology, crystallization and thermal behaviors of PLA-based composites: wonderful effects of hybrid GO/PEG via dynamic impregnating. *Polymers (Basel)*. 9:528. doi: 10.3390/polym9100528
- Jiang, W.-R., Bao, R.-Y., Yang, W., Liu, Z.-Y., Xie, B.-H., and Yang, M.-B. (2014). Morphology, interfacial and mechanical properties of polylactide/poly(ethylene terephthalate glycol) blends compatibilized by polylactide-g-maleic anhydride. *Mater. Des.* 59, 524–531. doi: 10.1016/j.matdes.2014.03.016
- Krishnan, S., Pandey, P., Mohanty, S., and Nayak, S. K. (2016). Toughening of polylactic acid: an overview of research progress. *Polym. Plast. Technol. Eng.* 55, 1623–1652. doi: 10.1080/03602559.2015.1098698
- Kucharczyk, P., Sedlarik, V., Miskolczi, N., Szakacs, H., and Kitano, T. (2012). Properties enhancement of partially biodegradable polyamide/polylactide blends through compatibilization with novel polyalkenyl-poly-maleic-anhydride-amide/imide-based additives. *J. Reinf. Plast. Compos.* 31, 189–202. doi: 10.1177/0731684411434150
- Kuzmanović, M., Delva, L., Mi, D., Martins, C., Cardon, L., and Ragaert, K. (2018). Development of crystalline morphology and its relationship with mechanical properties of PP/PET microfibrillar composites containing POE and POE-g-MA. *Polymers (Basel)*. 10:291. doi: 10.3390/polym10030291
- Lasprilla, A. J. R., Martinez, G. A. R., Lunelli, B. H., Jardini, A. L., and Filho, R. M. (2012). Poly-lactic acid synthesis for application in biomedical devices — a review. *Biotechnol. Adv.* 30, 321–8. doi: 10.1016/j.biotechadv.2011.06.019

DATA AVAILABILITY STATEMENT

All datasets generated for this study are included in the article/supplementary material.

AUTHOR CONTRIBUTIONS

AR, CS, and KP planned the conceptualization and design of the study. AR carried out the experiments and characterizations of the materials and wrote the first draft of the manuscript. All authors contributed to manuscript revision and read and approved the submitted version.

ACKNOWLEDGMENTS

We are gratefully acknowledge the International Campus on Safety and Intermodality in Transportation (CISIT, France), the European Community (FEDER funds), as well as the Hauts-de-France Region (France) for their contributions to funding extrusion equipment and characterization tools (dynamic rheometers, microscopes, goniometers, calorimeters, and tensile benches).

- Li, Z., Tan, B. H., Lin, T., and He, C. (2016). Recent advances in stereocomplexation of enantiomeric PLA-based copolymers and applications. *Prog. Polym. Sci.* 62, 22–72. doi: 10.1016/j.progpolymsci.2016.05.003
- Liu, H., and Zhang, J. (2011). Research progress in toughening modification of poly(lactic acid). *J. Polym. Sci. B Polym. Phys.* 49, 1051–1083. doi: 10.1002/polb.22283
- Lopes, M. S., Jardini, A. L., and Filho, R. M. (2012). Poly (lactic acid) production for tissue engineering applications. *Procedia Eng.* 42, 1402–1413. doi: 10.1016/j.proeng.2012.07.534
- Madhavan Nampoothiri, K., Nair, N. R., and John, R. P. (2010). An overview of the recent developments in polylactide (PLA) research. *Bioresour. Technol.* 101, 8493–8501. doi: 10.1016/j.biortech.2010.05.092
- Mantia, F., Ceraulo, M., Giacchi, G., Mistretta, M., and Botta, L. (2017). Effect of a compatibilizer on the morphology and properties of polypropylene/polyethyleneterephthalate spun fibers. *Polymers (Basel)*. 9:47. doi: 10.3390/polym9020047
- Mecking, S. (2004). Nature or petrochemistry?—biologically degradable materials. *Angew. Chemie Int. Ed.* 43, 1078–1085. doi: 10.1002/anie.200301655
- Mishra, J., Tiwari, S. K., Abolhasani, M. M., Azimi, S., and Nayak, G. C. (2017). “Fundamental of polymer blends and its thermodynamics,” in *Micro and Nano Fibrillar Composites (MFCs and NFCs) From Polymer Blends*, eds S. Thomas, R. Mishra, and N. Kalarikkal (Dhanbad: Elsevier), 27–55. doi: 10.1016/B978-0-08-101991-7.00002-9
- Mülhaupt, R. (2013). Green polymer chemistry and bio-based plastics: dreams and reality. *Macromol. Chem. Phys.* 214, 159–174. doi: 10.1002/macp.201200439
- Nagarajan, V., Mohanty, A. K., and Misra, M. (2016). Perspective on polylactic acid (PLA) based sustainable materials for durable applications: focus on toughness and heat resistance. *ACS Sustain. Chem. Eng.* 4, 2899–2916. doi: 10.1021/acssuschemeng.6b00321
- Nofar, M., Sacligil, D., Carreau, P. J., Kamal, M. R., and Heuzey, M.-C. (2019). Poly (lactic acid) blends: processing, properties and applications. *Int. J. Biol. Macromol.* 125, 307–360. doi: 10.1016/j.ijbiomac.2018.12.002
- Nuzzo, A., Coiai, S., Carroccio, S. C., Dintcheva, N. T., Gambarotti, C., and Filippone, G. (2014). Heat-resistant fully bio-based nanocomposite blends based on poly(lactic acid). *Macromol. Mater. Eng.* 299, 31–40. doi: 10.1002/mame.201300051
- Ogunniran, E. S., Sadiku, R., Sinha Ray, S., and Luruli, N. (2012). Morphology and thermal properties of compatibilized PA12/PP blends with boehmite alumina nanofiller inclusions. *Macromol. Mater. Eng.* 297, 627–638. doi: 10.1002/mame.201100254
- Pai, F.-C., Chu, H.-H., and Lai, S.-M. (2019). Preparation and properties of thermally conductive PLA/PA 610 biomass composites. *J. Elastomers Plast.* 52:0095244318825286. doi: 10.1177/0095244318825286
- Pai, F.-C., Lai, S.-M., and Chu, H.-H. (2013). Characterization and properties of reactive poly(lactic acid)/polyamide 610 biomass blends. *J. Appl. Polym. Sci.* 130, 2563–2571. doi: 10.1002/app.39473
- Pang, X., Zhuang, X., Tang, Z., and Chen, X. (2010). Polylactic acid (PLA): research, development and industrialization. *Biotechnol. J.* 5, 1125–1136. doi: 10.1002/biot.201000135
- Patel, R., Ruehle, D. A., Dorgan, J. R., Halley, P., and Martin, D. (2014). Biorenewable blends of polyamide-11 and polylactide. *Polym. Eng. Sci.* 54, 1523–1532. doi: 10.1002/pen.23692
- Pawar, R. P., Tekale, S. U., Shisodia, S. U., Totre, J. T., and Domb, A. J. (2014). Biomedical applications of poly(lactic acid). *Recent Pat. Regen. Med.* 4, 40–51. doi: 10.2174/2210296504666140402235024
- Quintana, R., Persenaire, O., Lemmouchi, Y., Bonnaud, L., and Dubois, P. (2016). Compatibilization of co-plasticized cellulose acetate/water soluble polymers blends by reactive extrusion. *Polym. Degrad. Stab.* 126, 31–38. doi: 10.1016/j.polymdegradstab.2015.12.023
- Raj, A., Prashantha, K., and Samuel, C. (2019). Compatibility in biobased poly(L-lactide)/polyamide binary blends: from melt-state interfacial tensions to (thermo)mechanical properties. *J. Appl. Polym. Sci.* 137:48440. doi: 10.1002/app.48440
- Rashmi, B. J., Prashantha, K., Lacrampe, M.-F., and Krawczak, P. (2015). Toughening of poly(lactic acid) without sacrificing stiffness and strength by melt-blending with polyamide 11 and selective localization of halloysite nanotubes. *Express Polym. Lett.* 9, 721–735. doi: 10.3144/expresspolymlett.2015.67
- Rasselet, D., Caro-Bretelle, A.-S., Taguet, A., and Lopez-Cuesta, J.-M. (2019). Reactive compatibilization of PLA/PA11 blends and their application in additive manufacturing. *Materials (Basel)*. 12:485. doi: 10.3390/ma12030485
- Saeidlou, S., Huneault, M. A., Li, H., and Park, C. B. (2012). Poly(lactic acid) crystallization. *Prog. Polym. Sci.* 37, 1657–1677. doi: 10.1016/j.progpolymsci.2012.07.005
- Samuel, C., Jean-Marie Raquez, P. D. (2013). PLLA/PMMA blends: a shear-induced miscibility with tunable morphologies and properties? *Polymer (Guildf)*. 54, 3931–3939. doi: 10.1016/j.polymer.2013.05.021
- Shi, X., Zhang, G., Phuong, T., and Lazzeri, A. (2015). Synergistic effects of nucleating agents and plasticizers on the crystallization behavior of poly(lactic acid). *Molecules* 20, 1579–1593. doi: 10.3390/molecules20011579
- Spinella, S., Samuel, C., Raquez, J.-M., McCallum, S. A., Gross, R., and Dubois, P. (2016). Green and efficient synthesis of dispersible cellulose nanocrystals in biobased polyesters for engineering applications. *ACS Sustain. Chem. Eng.* 4, 2517–2527. doi: 10.1021/acssuschemeng.5b01611
- Srithep, Y., Nealey, P., and Turng, L.-S. (2013). Effects of annealing time and temperature on the crystallinity and heat resistance behavior of injection-molded poly(lactic acid). *Polym. Eng. Sci.* 53, 580–588. doi: 10.1002/pen.23304
- Stoclet, G., Seguela, R., and Lefebvre, J.-M. (2011). Morphology, thermal behavior and mechanical properties of binary blends of compatible biosourced polymers: polylactide/polyamide11. *Polymer (Guildf)*. 52, 1417–1425. doi: 10.1016/j.polymer.2011.02.002
- Takemori, M. T. (1979). Towards an understanding of the heat distortion temperature of thermoplastics. *Polym. Eng. Sci.* 19, 1104–1109. doi: 10.1002/pen.760191507
- Tan, B. H., Muiruri, J. K., Li, Z., and He, C. (2016). Recent progress in using stereocomplexation for enhancement of thermal and mechanical property of polylactide. *ACS Sustain. Chem. Eng.* 4, 5370–5391. doi: 10.1021/acssuschemeng.6b01713
- Utracki, L. A., and Wilkie, C. A. (2014). *Polymer Blends Handbook*. Dordrecht: Springer. doi: 10.1007/978-94-007-6064-6
- Walha, F., Lamnawar, K., Maaouz, A., Jaziri, M., Walha, F., Lamnawar, K., et al. (2016). Rheological, morphological and mechanical studies of sustainably sourced polymer blends based on poly(lactic acid) and polyamide 11. *Polymers (Basel)*. 8:61. doi: 10.3390/polym8030061
- Wang, N., Yu, J., and Ma, X. (2007). Preparation and characterization of thermoplastic starch/PLA blends by one-step reactive extrusion. *Polym. Int.* 56, 1440–1447. doi: 10.1002/pi.2302
- Wang, Y.-L., Hu, X., Li, H., Ji, X., and Li, Z.-M. (2010). Polyamide-6/poly(lactic acid) blends compatibilized by the maleic anhydride grafted polyethylene-octene elastomer. *Polym. Plast. Technol. Eng.* 49, 1241–1246. doi: 10.1080/03602559.2010.496418
- Zeng, J.-B., Li, K.-A., and Du, A.-K. (2015). Compatibilization strategies in poly(lactic acid)-based blends. *RSC Adv.* 5, 32546–32565. doi: 10.1039/C5RA01655J
- Zhang, M., and Thomas, N. L. (2011). Blending polylactic acid with polyhydroxybutyrate: the effect on thermal, mechanical, and biodegradation properties. *Adv. Polym. Technol.* 30, 67–79. doi: 10.1002/adv.20235

Conflict of Interest: The authors declare that the research was conducted in the absence of any commercial or financial relationships that could be construed as a potential conflict of interest.

Copyright © 2020 Raj, Samuel and Prashantha. This is an open-access article distributed under the terms of the Creative Commons Attribution License (CC BY). The use, distribution or reproduction in other forums is permitted, provided the original author(s) and the copyright owner(s) are credited and that the original publication in this journal is cited, in accordance with accepted academic practice. No use, distribution or reproduction is permitted which does not comply with these terms.